

# Aggregates in Solution of Binary Mixtures of Amphiphilic Diblock Copolymers with Different Chain Length

Xuan Li, Ping Tang,\* Feng Qiu, Hongdong Zhang, and Yuliang Yang\*

Key Laboratory of Molecular Engineering of Polymer, Ministry of Education, and Department of Macromolecular Science, Fudan University, Shanghai 200433, China

Received: October 18, 2005; In Final Form: December 8, 2005

The polydispersity effect of amphiphilic AB diblock copolymers on the self-assembled morphologies in solution has been investigated by the real-space implementation of self-consistent field theory (SCFT) in two dimensions (2D). The polydispersity is artificially obtained by mixing binary diblock copolymers where the hydrophilic or hydrophobic blocks are composed of two different lengths while the other block length is kept the same. The main advantage is that this simple polydispersity can easily distinguish the difference of aggregates in the density distribution of long and short block length intuitively and quantitatively. The morphology transition from vesicles to micelles is observed with increasing polydispersity of copolymers due to the length segregation of copolymers. For polydisperse hydrophilic or hydrophobic blocks, the short blocks tend to distribute at the interfaces between hydrophilic and hydrophobic blocks while the long blocks stretch to the outer space. More specifically, by quantitatively taking the sum of all the concentration distribution of long and short chains over the inside and outside surface areas of the vesicle, it is found that long blocks prefer to locate on the outside surface of the vesicle while short ones prefer the inside. Such length segregation leads to large curvature of the aggregate, thus resulting in the decrease of the aggregate size.

## Introduction

It has been known for many years that asymmetric, amphiphilic, block copolymers can self-assemble in selective solvents to form aggregates of various morphologies,<sup>1</sup> such as spherical micelles, micellar rods, bilayers (lamellae and vesicles), tubules, large compound micelles (LCMs), hexagonally packed hollow hoops, etc.<sup>2–5</sup> The aggregate morphologies have been receiving much attention both experimentally and theoretically in recent years due to many potential applications such as drug delivery, the cosmetic industry, and encapsulation technologies.<sup>6–10</sup>

Despite a number of experimental studies that have been carried out to investigate the aggregates including vesicles in solution, the theoretical work on the complex microstructures of block copolymers in solution is relatively scarce. In the past years, a variety of theoretical approaches, including Monte Carlo simulation,<sup>11,12</sup> Brownian dynamic simulations,<sup>13</sup> and dissipative particle dynamics,<sup>14</sup> have played significant roles in the investigation of formation of various complex morphologies. Another approach for this investigation is self-consistent field theory (SCFT). For periodic systems, the Fourier space implementation of the SCFT proposed by Matsen and Schick is effective and precise, and has been applied for AB diblock copolymer with A homopolymer blends that form micelles.<sup>15</sup> However, the method is not best suited for studying the vesicles that do not form periodic structures.<sup>16</sup> For nonperiodic systems, real-space implemented SCFT proposed by Drolet and Fredrickson<sup>17–19</sup> is frequently used to explore the self-assembled morphologies of complex multiblock copolymers in bulk.<sup>20,21</sup> Recently, such a method has been extended to investigate the aggregation of AB diblock copolymers in solution by Liang et

al.,<sup>22</sup> and ABC linear triblock copolymers in solution by our group in our previous paper.<sup>23</sup> By tailoring the interaction parameters and the initial fluctuation, circular micelles, linear micelles, and vesicles (corresponding to spherulike micelles, rodlike micelles, and vesicles in 3D space) were obtained. Actually the practical applications of aggregates of block copolymers in solution depend on the specific morphology of aggregates. Following Eisenberg's idea, the aggregation of block copolymers depends on three contributions to the free energy of the system, namely chain stretching in the core, the interfacial energy, and repulsion among corona chains.<sup>6,24</sup> Among the factors that control the shape and size of aggregates, despite the block ratio and interaction parameters being fairly well understood,<sup>25</sup> the effect of polydispersity of block copolymers on the aggregation is less touched. However, practical synthetic polymers are mostly polydisperse, which is intrinsic in polymerization. Especially, the recent controlled free radical polymerization has been explored to prepare block copolymers because of the low cost and high efficiency in synthesizing copolymers with well-defined compositions and complex architectures compared to the traditional anionic polymerization. Unfortunately, the resulting copolymers frequently have somewhat broader molecular weight distributions (polydispersities) relative to, for example, living anionic techniques. To take advantage of these cheaper and newer copolymers, it is necessary to investigate the effect of polydispersity on the aggregation behavior.

Only a few studies have been taken to investigate the effect of polydispersity on block copolymer self-assembly experimentally and theoretically.<sup>26</sup> Fredrickson studied the effect of polydispersity on the bulk phase behavior of block copolymer melts.<sup>27,28</sup> Matsen and Bates investigated the effect of polydispersity originating from binary diblock copolymer blends with different length on the phase behavior in bulk.<sup>29,30</sup> Very recently

\* Address correspondence to these authors. E-mail: pingtang@fudan.edu.cn (P.T.) and ylyang@srcap.stc.sh.cn (Y.L.Y.).

the effect of the polydispersity of AB diblock copolymers on the aggregates in solution was investigated by real-space implementation of SCFT in 2D.<sup>31</sup> However, they examined the density distribution of different chain length from the  $n_g$ -point Gaussian quadratures adopted to describe the continuous length distribution, and thereby this method cannot really quantitatively and directly differentiate where long chains or short chains were. In this paper, to quantitatively elucidate, in polydisperse copolymers, the segregation according to long and short chain lengths, the intuitive and efficient way is to obtain the polydispersity by mixing two AB diblock copolymers with different lengths. By means of this artificial polydispersity, quantitative concentration distribution of long and short chains on the inside and outside of a vesicle can be easily figured out by using 2D real-space implementation of SCFT.

We note that the computational cost of 3D simulation limits the 3D real space SCF implementation and most of the previous work was carried out in 2D. Following Fredrickson's idea of real-space implementation SCFT,<sup>27,28</sup> we start from a random uniform distribution initial density profile and let the system evolve to equilibrium in 2D lattice space. It is noted that the resulting aggregates largely depend on the initial fluctuation amplitude, possibly corresponding to different experimental preparation conditions, such as the concentration and quenching temperature. As a result, our simulation is performed using the same initial fluctuation amplitude value on the order of  $10^{-4}$  with random uniform distribution to ensure that these obtained different morphologies are not influenced by the initial condition. Furthermore, all the simulation is repeated at least 10 times with different random states and different random numbers to guarantee the structure is not occasionally observed.

### Theoretical Method

Consider the SCFT for a mixture of  $n_p$  binary AB diblock copolymer blends with  $n_s$  solvent molecules confined to a volume  $V$ . The block copolymer mixtures are obtained by blending binary block copolymers with different hydrophilic (hydrophobic) block lengths but the same hydrophobic (hydrophilic) length to artificially increase the polydispersity index (PI) of copolymers. Here, for clarity, we assume the hydrophilic blocks A are the mixtures of two different chain lengths: the first chain consists of  $N_1$  ( $N_1 = N_{A1} + N_B$ ) and the second chain  $N_2$  ( $N_2 = N_{A2} + N_B$ ) average Gaussian coarse-grained segments, each having equal statistical segment length  $a$ . The number percentage of different chain lengths is  $P_{N_1}$  for  $N_1$  and  $P_{N_2}$  ( $P_{N_2} = 1 - P_{N_1}$ ) for  $N_2$ , respectively. The composition (average volume fractions) of species A in binary copolymer blends is  $f_A = (N_{A1}P_{N_1} + N_{A2}P_{N_2})/(N_1P_{N_1} + N_2P_{N_2}) = (N_{A1}P_{N_1} + N_{A2}P_{N_2})/\bar{N}$  ( $f_{A1} = N_{A1}P_{N_1}/\bar{N}$  and  $f_{A2} = f_A - f_{A1}$ ) and  $f_B = 1 - f_A$ , respectively.  $\bar{N}$  is the number average chain length of block copolymer blends,  $\bar{N} = N_1P_{N_1} + N_2P_{N_2}$ . We assume the mixture is incompressible with each polymer segment occupying a fixed volume  $\rho_0^{-1}$  and each solvent molecule taking the same volume  $v_s = \rho_0^{-1}$ . Therefore, the total volume of the system is  $V = n_p\bar{N}/\rho_0 + n_s v_s$ , the volume fraction of block copolymers in solution is  $f_p = n_p\bar{N}/V\rho_0$ , and that of the solvent is  $f_s = 1 - f_p$  because of the incompressibility condition.

In the SCFT, the many interacting chains are reduced to that of independent chains subject to a set of effective chemical potential fields  $w_i$  created by the other chains, where  $i$  represents block species A, B, or solvent S. These chemical potential fields, which represent the actual interactions between different components, are conjugated to the segment density fields,  $\phi_i$ , of different species  $i$ . Hence, the free energy (in units of  $k_B T$ )

of the system is given by

$$F = -f_p f_{A1} \ln(Q_1/V) - f_p f_{A2} \ln(Q_2/V) - \bar{N} f_s \ln(Q_s/V) - 1/V \int d\mathbf{r} [w_A \phi_A + w_B \phi_B + w_S \phi_S + \xi(1 - \phi_A - \phi_B - \phi_S)] + 1/V \int d\mathbf{r} [\chi_{AB} \bar{N} \phi_A \phi_B + \chi_{AS} \bar{N} \phi_A \phi_S + \chi_{BS} \bar{N} \phi_B \phi_S] \quad (1)$$

where  $\chi_{ij}$  is the Flory–Huggins interaction parameter between species  $i$  and  $j$ ,  $\xi$  is the Lagrange multiplier (as a pressure), and  $Q_1 = \int d\mathbf{r} q(\mathbf{r}, N_1)$  and  $Q_2 = \int d\mathbf{r} q(\mathbf{r}, N_2)$  are the partition function of a single chain in the effective chemical potential fields  $w_A$  and  $w_B$ .  $Q_s = \int d\mathbf{r} \exp(-w_S(\mathbf{r})/\bar{N})$  is the partition function of the solvent in the effective chemical potential field  $w_S$ . The fundamental quantity to be calculated in mean-field studies is the polymer segment probability distribution function,  $q(\mathbf{r}, s)$ , representing the probability of finding segment  $s$  at position  $\mathbf{r}$ . It satisfies a modified diffusion equation using a flexible Gaussian chain model:<sup>32,33</sup>

$$\frac{\partial}{\partial s} q(\mathbf{r}, s) = \frac{\bar{N} a^2}{6} \nabla^2 q(\mathbf{r}, s) - w q(\mathbf{r}, s) \quad (2)$$

where  $w$  is  $w_A$  when  $0 < s < f_A$ , and  $w_B$  when  $f_A < s < f_B$ . The initial condition of eq 2 satisfies  $q(\mathbf{r}, 0) = 1$ . Because the two ends of the block copolymer are different, a second distribution function  $q^+(\mathbf{r}, s)$  is needed, which satisfies eq 2 but with the right-hand side multiplied by  $-1$  and the initial condition  $q^+(\mathbf{r}, 1) = 1$ . The density of each component is thus obtained by

$$\phi_A(\mathbf{r}) = f_p V \left[ \frac{1}{Q_1 N_1} \int_0^{f_{A1} N_1} ds q(\mathbf{r}, s) q^+(\mathbf{r}, s) + \frac{1}{Q_2 N_2} \int_0^{f_{A2} N_2} ds q(\mathbf{r}, s) q^+(\mathbf{r}, s) \right] \quad (3)$$

$$\phi_B(\mathbf{r}) = f_p V \left[ \frac{1}{Q_1 N_1} \int_{f_{A1} N_1}^{N_1} ds q(\mathbf{r}, s) q^+(\mathbf{r}, s) + \frac{1}{Q_2 N_2} \int_{f_{A2} N_2}^{N_2} ds q(\mathbf{r}, s) q^+(\mathbf{r}, s) \right] \quad (4)$$

$$\phi_S(\mathbf{r}) = \frac{f_s V}{Q_s} \exp(-w_S(\mathbf{r})/\bar{N}) \quad (5)$$

Minimization of the free energy with respect to density and pressure, namely,  $\delta F/\delta \phi = \delta F/\delta \xi = 0$ , leads to the following equations.

$$w_A(\mathbf{r}) = \chi_{AB} \bar{N} \phi_B(\mathbf{r}) + \chi_{AS} \bar{N} \phi_S(\mathbf{r}) + \xi(\mathbf{r}) \quad (6)$$

$$w_B(\mathbf{r}) = \chi_{AB} \bar{N} \phi_A(\mathbf{r}) + \chi_{BS} \bar{N} \phi_S(\mathbf{r}) + \xi(\mathbf{r}) \quad (7)$$

$$w_S(\mathbf{r}) = \chi_{AS} \bar{N} \phi_A(\mathbf{r}) + \chi_{BS} \bar{N} \phi_B(\mathbf{r}) + \xi(\mathbf{r}) \quad (8)$$

$$\phi_A(\mathbf{r}) + \phi_B(\mathbf{r}) + \phi_S(\mathbf{r}) = 1 \quad (9)$$

Here we solve eqs 3–9 directly in real space by using a combinatorial screening algorithm proposed by Drolet and Fredrickson.<sup>17,18</sup> The algorithm consists of randomly generating the initial values of the fields  $w_i(\mathbf{r})$ . By using a Crank–Nicholson scheme and an alternating–direct implicit (ADI) method<sup>13</sup> the diffusion equations are then integrated to obtain  $q$  and  $q^+$ , for  $0 < s < 1$ . Next, the right-hand sides of eqs 3–5 are evaluated to obtain new values for the volume fractions of blocks A and B and solvent S.

**TABLE 1: AB Diblock Copolymer Binary Blends with Different PI of Hydrophilic Block A but Monodisperse Block B**

| blends | copolymer 1 (%)                     | copolymer 2 (%)                      | PI of block A |
|--------|-------------------------------------|--------------------------------------|---------------|
| 1      | A <sub>3</sub> B <sub>24</sub> (50) | A <sub>3</sub> B <sub>24</sub> (50)  | 1.00          |
| 2      | A <sub>2</sub> B <sub>24</sub> (75) | A <sub>6</sub> B <sub>24</sub> (25)  | 1.33          |
| 3      | A <sub>1</sub> B <sub>24</sub> (50) | A <sub>5</sub> B <sub>24</sub> (50)  | 1.44          |
| 4      | A <sub>1</sub> B <sub>24</sub> (67) | A <sub>7</sub> B <sub>24</sub> (33)  | 1.89          |
| 5      | A <sub>1</sub> B <sub>24</sub> (78) | A <sub>10</sub> B <sub>24</sub> (22) | 2.56          |

The numerical simulations are carried out on the 2D space with  $150 \times 150$  square lattice. The grid size is  $\Delta x = 0.5$ . The simulation is carried out until the phase patterns are stable and the free energy difference between two iterations is smaller than  $10^{-5}$ .

It should be noted that the mean-field approximation is known to be inaccurate when the concentration fluctuation is large. Therefore, regarding the application of SCFT to copolymer solution the concentration of copolymers requires no less than 0.1. Furthermore, to decrease the influence of the concentration fluctuation the chain length may take relatively short values, such as less than 40, but too short a length will also cause the mean-field approximation to fail. In fact in such instances, a new accurate method for numerically sampling the concentration fluctuation is required and is still a challenging task.<sup>19</sup>

## Results and Discussion

To study the effect of polydispersity of block copolymers on the aggregate structure in solution, we simply mix two copolymers with different chain length to artificially broaden the PI of block copolymers, as Eisenberg and co-workers did experimentally.<sup>9,10</sup> In our simulation, the average chain length is assumed as 27 and the average block ratio is fixed to be a hydrophilic/hydrophobic block length of 3/24, noted as A<sub>3</sub>B<sub>24</sub>, namely the hydrophilic block A with an average block length of 3 and the hydrophobic block B with an average block length of 24. In this case, the block copolymer forms the so-called crew-cut aggregates. The concentration of block copolymers is set as  $f_p = 0.1$  to ensure that the concentration of the polymer is low. Therefore the volume fraction of hydrophilic block A, hydrophobic block B, and solvent S is  $f_A = 0.011$ ,  $f_B = 0.089$ , and  $f_S = 0.9$ , respectively. The interaction parameters are set to be following values:  $\chi_{AB}\bar{N} = 22$ ,  $\chi_{AS}\bar{N} = -1$ , and  $\chi_{BS}\bar{N} = 26$  in all simulations, except for  $\chi_{AB}\bar{N} = 31.3$  in Figure 4, and thus the A block is hydrophilic while the B block is hydrophobic. For simplicity, one of the block species in the block copolymer is assumed to be polydisperse, while another is assumed to be monodisperse. In the following, the two classes are investigated in terms of the polydispersity of hydrophilic and hydrophobic blocks.<sup>19</sup>

**A. Hydrophilic Blocks Are Composed of Blocks of Two Different Lengths.** Two diblock copolymers with different lengths of hydrophilic block A and a constant length of hydrophobic block B are mixed to artificially broaden the hydrophilic block length distribution. Table 1 presents a series of mixture contents and the resulting PI of hydrophilic block A.

The aggregate morphologies with an increase of hydrophilic block PI are shown in Figure 1. The morphology is presented with different colors, where red and blue are assigned to A and B blocks, respectively, and the rest are solvents. In Figure 1, as the PI of hydrophilic blocks increases, the morphology in dilute solution changes first from vesicles to the mixture of vesicles, circle-like micelles corresponding to sphere-like micelles in 3D and rods, then to vesicles along with circle-like micelles, and finally only large compound micelles (LCMs). Obviously,

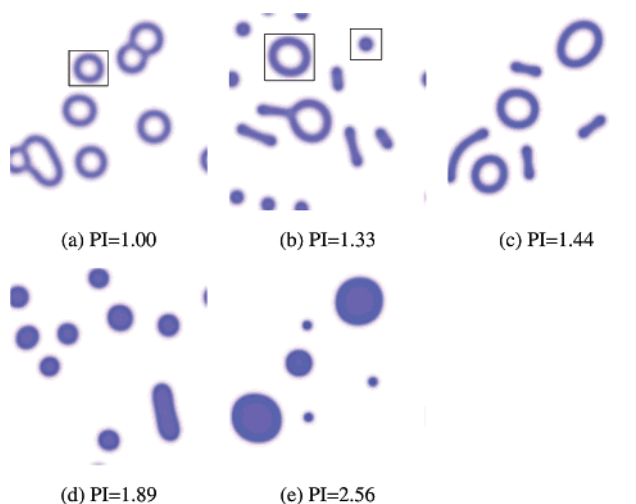


**Figure 1.** Aggregate morphologies in dilute solution of amphiphilic diblock copolymer blends as prepared in Table 1 with an increase of PI of hydrophilic block A.

vesicles disappear while micelles are found instead with further increasing PI of hydrophilic block A. To look into the structure information of the aggregates in detail, first for vesicles the density distribution profile of hydrophilic block, hydrophobic block, and the solvent is plotted in Figure 2.

The denoted “C” and “W” dotted lines represent the center of the vesicle and the center of the bilayer wall, corresponding to the density peaks of the solvents and the hydrophobic block, respectively. From Figure 2 (top), it is clearly seen that the hydrophobic block distribution in the vesicle shows a typical bimodal mark, which is characteristic of a vesicle regardless of the hydrophilic block PI. In the bottom of Figure 2, the basic building unit of a vesicle is a bilayer comprising inner and outer leafs, where hydrophilic block A lies in the inner and outer side surfaces of the vesicle in contact with the solvent directly. It should be emphasized that the density peak of the hydrophilic block on the inner side surface of the vesicle is always higher than that on the outside. It is a common phenomenon that due to the curvature of the vesicle the outside leaf has more space for polymer chain stretching, while on the inside, chains should be packed up, and thus lead to higher density distribution near the inner wall than the outside. Furthermore, for the vesicle formed by polydisperse hydrophilic blocks, corresponding to the blank marked vesicle in Figure 1b with PI = 1.33, the copolymer chains segregate in terms of different length. As shown in the bottom of Figure 2b, the short hydrophilic block tends to distribute at the interface between the long hydrophilic and hydrophobic block. This is in agreement with the simulation on diblock copolymer solution with continuous polydispersity blocks by Liang and co-workers.<sup>31</sup>

To quantitatively investigate whether long or short hydrophilic chains prefer to segregate to the inner or outer surface of a vesicle, we look into the overall concentration distribution of long and short hydrophilic blocks over the inner and outer surface areas of the vesicle, respectively. We sum up the concentration of two different lengths of hydrophilic chains inside and outside of the vesicle surface areas of the blank marked vesicle in Figure 1b with PI of 1.33. As mentioned above, due to the confined space at the inner leaf of the vesicle compared to the boarder space at the outer leaf of the vesicle, it is reasonable to compare the concentration ratio of short chains to long chains. On the outside surface of the vesicle, the concentration ratio of short chains to long chains is 1.44, while it is 1.66 on the inner side. Obviously, the short chain on the



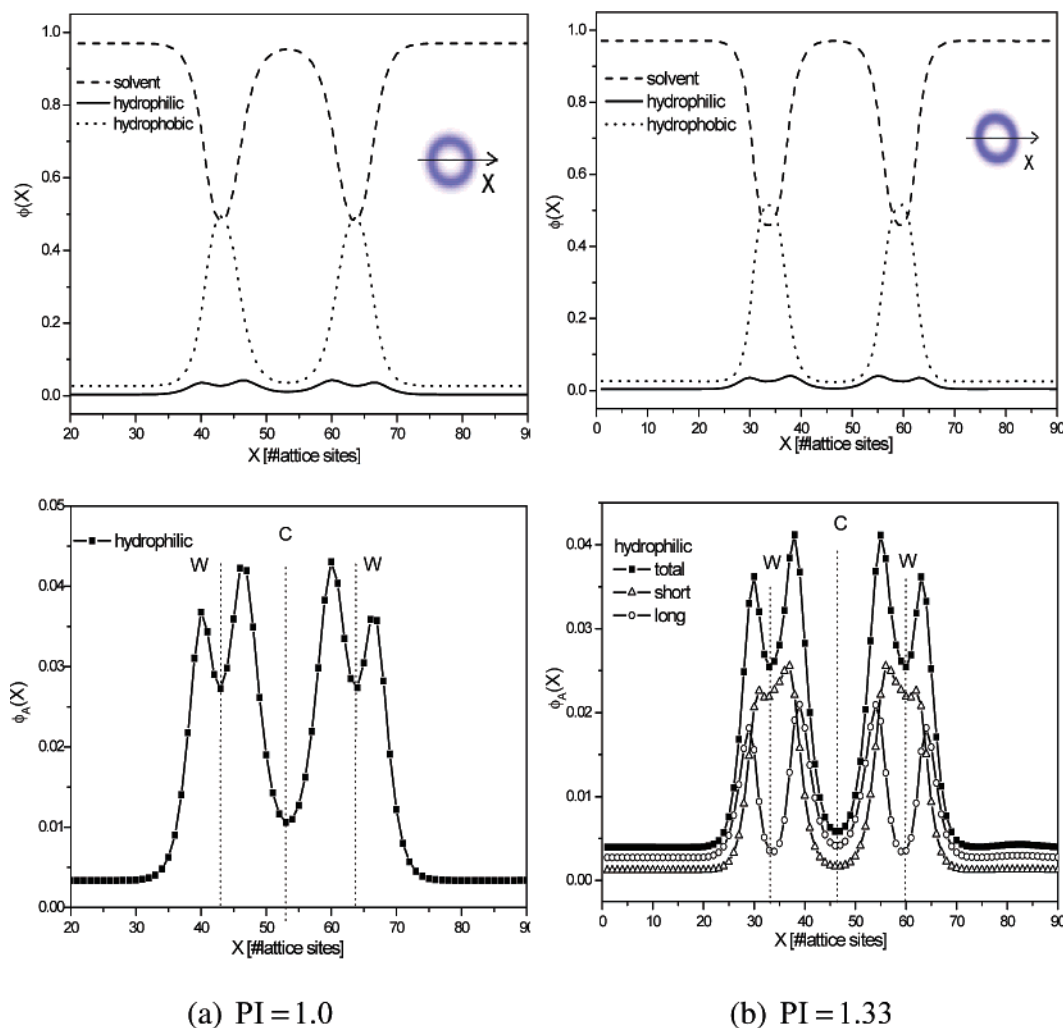


**Figure 2.** Density distribution of a vesicle blank marked in Figure 1, parts a and b, respectively, for polydisperse hydrophilic block A: PI = 1.0 (a) and 1.33 (b). Dotted lines with C and W denote the center of a vesicle and the center of the bilayer wall, respectively.

inner side of the vesicle maintains proportionally higher concentration than it does on the outer side of the vesicle, in other words, short hydrophilic chains preferentially segregate to the inner surface of the vesicle while long hydrophilic chains tend to segregate to the outside of the vesicle. Such a length segregation mechanism confirms Eisenberg's experimental observations in the mixture of diblock copolymers with different lengths.<sup>9</sup> Also, this segregation was observed in continuous polydisperse copolymer solution by Liang and co-workers.<sup>31</sup> As the PI of block copolymers increases, there are more long and short chains compared to the monodispersed copolymers. Since there are more short chains segregating to the inside of the vesicle and more long chains locating on the outside, this leads to the decrease of the average size of aggregates due to the repulsions among long chains and finally a morphological transition occurs from vesicle to micelles, LCMs. Actually, such length segregation can be distinguished more easily as the PI increases. As shown in Figure 3, with a further increase of the PI there are more long and short chains compared to the monodispersed copolymer, and thus more short chains prefer to stay on the inside. From the bottom of Figure 3, it is clearly seen that short chains locate on the inside of the so-called quasivesicle in Liang's notation while long chains completely extend to the outside forming the brush. Therefore, the tendency of short chains locating on the inside of the vesicle and long chains on the outside becomes more prominent with increased PI.

Interestingly, if we only increase the interaction parameter up to  $\chi_{AB}\bar{N} = 31.3$ , while the other parameters remain the same as in Figure 1b, compared to Figure 1b, very large vesicles are observed as shown in the inset of Figure 4 in order to decrease the interaction energy between blocks A and B. From Figure 4, it is again found that the short chains obviously distribute at the hydrophilic and hydrophobic block interfaces. However, the preferential segregation according to different length is quite different compared to small size vesicles in Figure 1b. In this case, the ratio of short chains to long chains on the inside is almost the same as that on the outside of the vesicle, namely long and short chains are more or less equally distributed on both sides of an extremely large vesicle. Contrary to the small size vesicle in Figure 1b, the large vesicle has small curvature, and especially along some cut lines shown in the inset of Figure 4, the bilayer of this part is nearly flat with the curvature approximately being zero. Therefore, the preferential segregation, namely having long chains segregate to the outside of the vesicle, while the short ones segregate to the inside, leads to the curvature of the aggregate formed. In other words, the curvature of the vesicles is stabilized by this preferential length segregation. At the same time, this length segregation induced spontaneous curvature causes the vesicle size to be changed. In fact, for polydisperse copolymers in solution, there exists a competition effect on the aggregate morphology between the repulsive interaction energy between different block species and

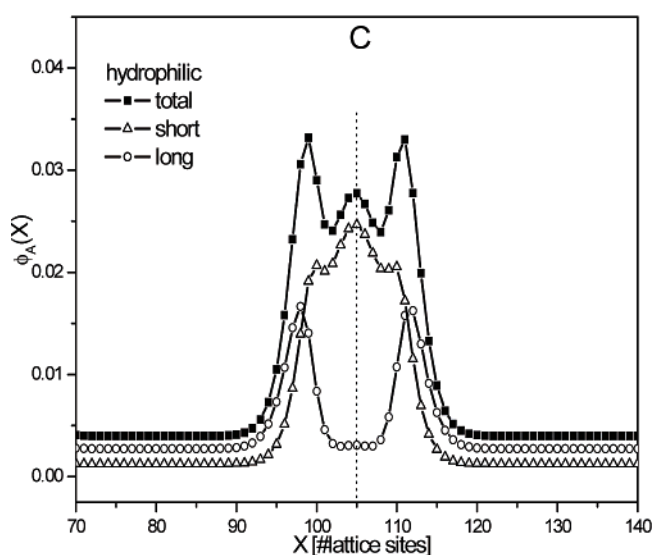
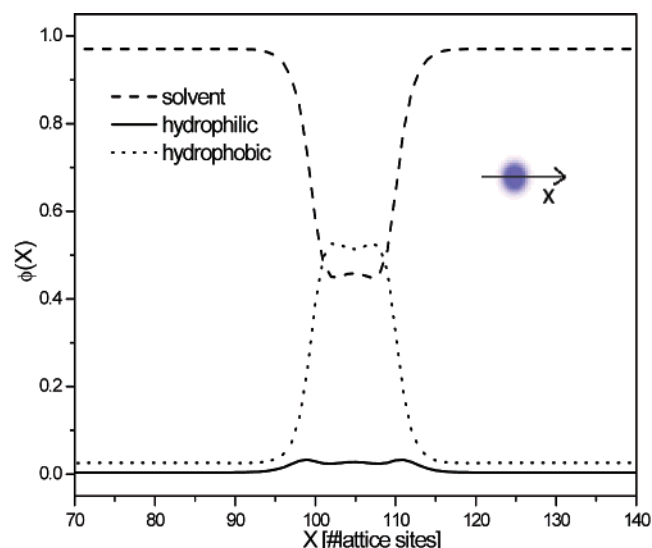


**Figure 3.** Density distribution profile of a quasivesicle blank marked in Figure 1b. The dotted line with C denotes the center of a vesicle.

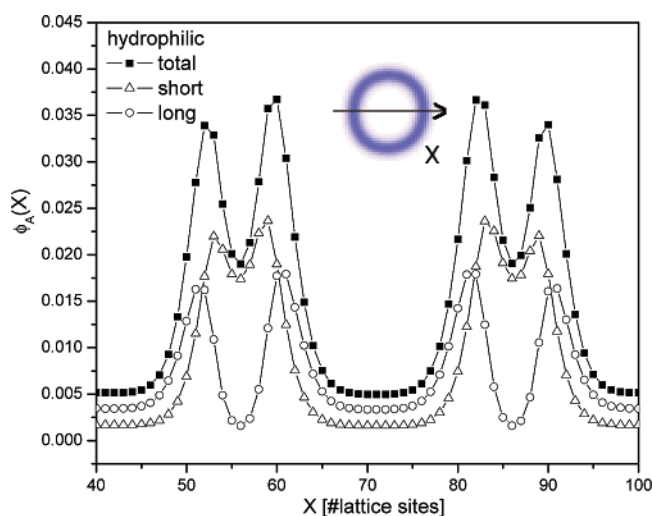


**Figure 4.** Density distribution of a large vesicle with hydrophilic block  $PI = 1.33$  and  $\chi_{AB}\bar{N} = 31.3$ .

the length segregation originating from the polydispersity. When the copolymer is in the weak or intermediate segregation regime, the preferential length segregation dominates and drives the

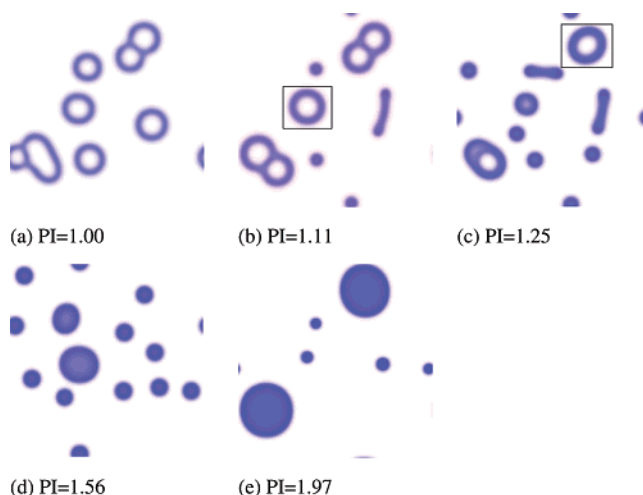


**Figure 5.** Aggregate morphologies in dilute solutions of amphiphilic diblock copolymer blends as prepared in Table 2 with an increase of PI of hydrophobic block B.

**TABLE 2: AB Diblock Copolymer Binary Blends with Different PI of Hydrophobic Block B but Monodisperse Block A**

| blends | copolymer 1 (%)                     | copolymer 2 (%)                     | PI of B block |
|--------|-------------------------------------|-------------------------------------|---------------|
| 1      | A <sub>3</sub> B <sub>24</sub> (50) | A <sub>3</sub> B <sub>24</sub> (50) | 1.00          |
| 2      | A <sub>3</sub> B <sub>16</sub> (50) | A <sub>3</sub> B <sub>32</sub> (50) | 1.11          |
| 3      | A <sub>3</sub> B <sub>6</sub> (31)  | A <sub>3</sub> B <sub>32</sub> (69) | 1.25          |
| 4      | A <sub>3</sub> B <sub>4</sub> (45)  | A <sub>3</sub> B <sub>40</sub> (55) | 1.56          |
| 5      | A <sub>3</sub> B <sub>4</sub> (58)  | A <sub>3</sub> B <sub>52</sub> (42) | 1.97          |

system to form small vesicles. On the contrary, when the copolymer is in the strong segregation regime, the interaction energy between different blocks becomes so large as to overwhelm the length segregation, thus leading to large vesicles and uniform distribution of long and short chains on both sides of the vesicle.

Furthermore, by investigating the concentration distribution of different lengths in different forms of aggregates, it is interesting to find that short chains like to remain vesicles and rod-like micelles while long chains prefer to form circle-like micelles.

**B. Polydisperse Hydrophobic Block.** In this subsection, we consider the case for polydisperse diblock copolymer mixtures made by two copolymers with different hydrophobic block B length but identical hydrophilic block length. A series of mixture contents and the resulting PI of hydrophobic block B are shown in Table 2.

The aggregate morphology with an increase of hydrophobic block PI is shown in Figure 5. As the PI of hydrophobic blocks increases, the morphology in dilute solution changes first from vesicles to the mixture of vesicles, spheres, and rods, then to coexistence of vesicles and spheres, and finally only large compound micelles (LCMs). Obviously, this is similar to the case of hydrophilic block polydispersity in Figure 1. To investigate the structure information of the aggregates in detail, the density distribution profile of hydrophilic block, hydrophobic block, and the solvent for the vesicles with different hydrophobic block PI is plotted in Figure 6.

Figure 6a (top and bottom) clearly shows that the short hydrophobic blocks tend to locate at the interfaces between hydrophilic and hydrophobic blocks, with two small peaks at the interfaces, while the longer chains extend to the outer surfaces, similar to the case of a polydisperse hydrophilic block. However, this situation is quite different when the hydrophobic block PI is further increased. As the PI of hydrophilic block B

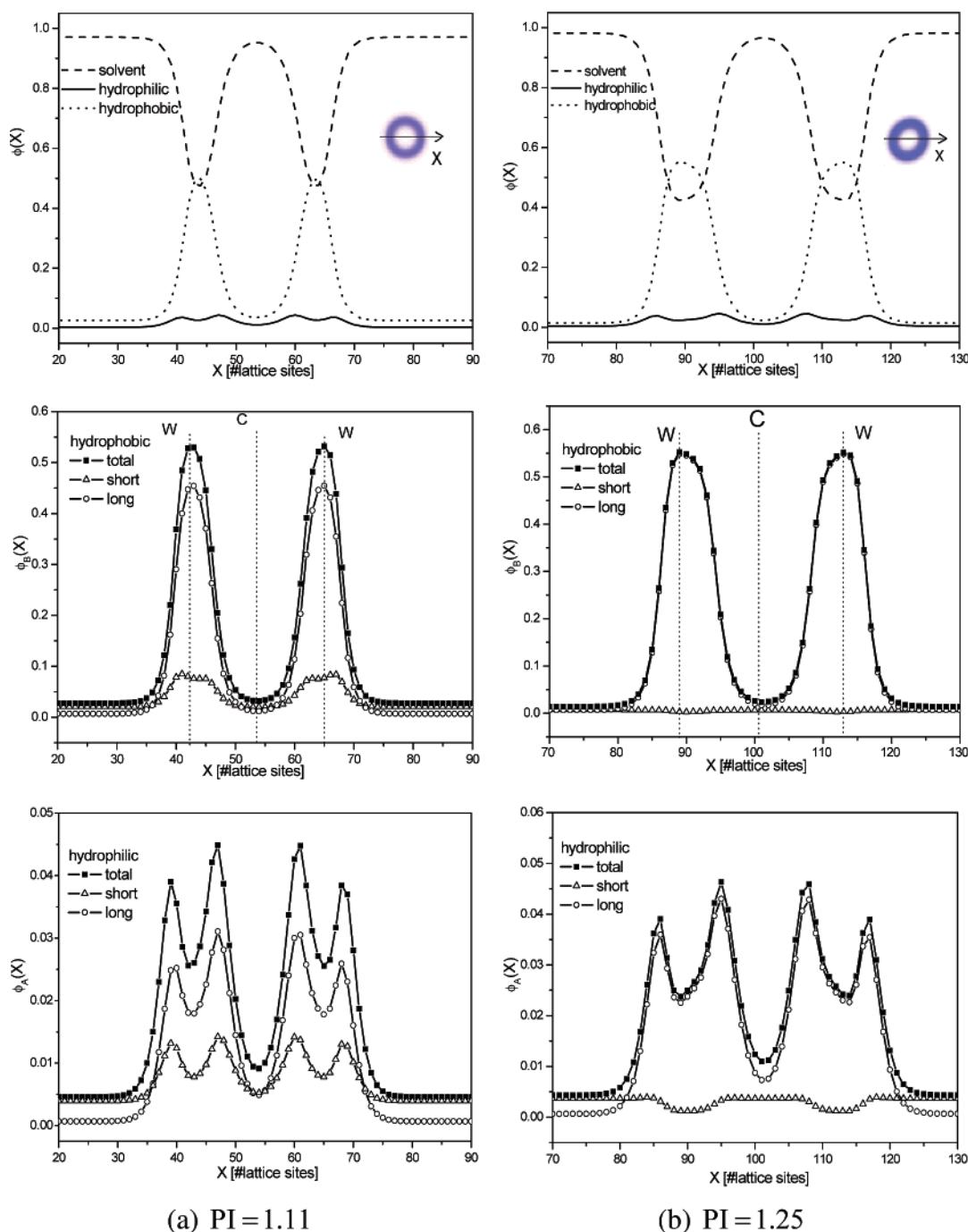


**Figure 6.** Density distribution of a vesicle blank marked in Figure 5, parts b and c, respectively, for polydisperse hydrophobic block B: PI = 1.11 (a) and 1.25 (b). Middle: Density contribution of two different hydrophobic lengths. Bottom: Density contribution of hydrophilic blocks with different hydrophobic length. Dotted lines with C and W denote the center of a vesicle and the center of the bilayer wall, respectively.

is further increased, up to  $PI = 1.25$ , compared to the case of  $PI = 1.11$ , there are much shorter hydrophobic blocks. From Figure 6b, the short hydrophobic blocks are slightly distributed at the hydrophilic/hydrophobic interfaces and are even almost distributed uniformly in the solution, and moreover, for short hydrophobic blocks, the hydrophilic blocks are more or less uniformly distributed. This indicates that the copolymers with a very short hydrophobic block act as hydrophilic homopolymers in solution.

## Summary

To conclude, we have applied 2D real-space self-consistent field theory to investigate the aggregation behavior of the

polydisperse diblock copolymers in dilute solution. For the sake of simplicity and quantitative prediction, the polydispersity is artificially acquired by mixing binary copolymer blends where one of the block species is composed of two different lengths while the other block length is kept the same. In this article, we discuss two cases: one is the polydisperse hydrophilic block copolymers, and the other is polydisperse hydrophobic copolymers. In both cases, the increase in PI leads to a variety of morphology changes from vesicles to the mixture of vesicles and micelles and finally to micelles due to the length segregation. The short blocks tend to segregate to the interfaces between hydrophilic and hydrophobic blocks while the long blocks prefer to extend to the outside of the aggregate. Especially, by

quantitatively summing up all the concentration distribution of long and short chains over the inside and outside surface areas of the vesicle, long blocks would rather segregate to the outside while short ones prefer the inside surface of the vesicle. Therefore, this length segregation existing in polydisperse block copolymers results in the decrease of the size of aggregates, in agreement with experimental and theoretical results. However, for high PI of hydrophobic blocks, the relatively short hydrophobic block copolymer behaves like a solvent-philic homopolymer. As a result, for short hydrophobic block copolymers, the hydrophobic block is slightly distributed at hydrophilic and hydrophobic interfaces and the hydrophilic block is almost uniformly distributed in the solvents.

**Acknowledgment.** The authors acknowledge financial support from the National Basic Research Program of China (Grant No. 2005CB623800) and the Excellent Research Group of NSF of China. The NSF of China (Grant Nos. 20474012, 20374016 and 20104002) is also acknowledged.

## References and Notes

- (1) Zhang, L. F.; Eisenberg, A. *Science* **1995**, 268, 1728.
- (2) Loppinet, B.; Sigel, R.; Larsen, A.; Fytas, G.; Vlassopoulos, D.; Liu, G. *Langmuir* **2000**, 16, 6480.
- (3) Schlaad, H.; Kukulka, H.; Smarsly, B.; Antonietti, M.; Pakula, T. *Polymer* **2002**, 43, 5321.
- (4) Becker, M. L.; Remsen, E. E.; Wooley, K. L. *J. Polym. Sci., Part A: Polym. Chem.* **2001**, 39, 4152.
- (5) Bailey, T. S.; Pham, H. D.; Bates, F. S. *Macromolecules* **2001**, 34, 6994.
- (6) Discher, D. E.; Eisenberg, A. *Science* **2002**, 297, 967.
- (7) Zhang, L. F.; Yu, K.; Eisenberg, A. *Science* **1996**, 272, 1777.
- (8) Choucair, A. A.; Kycia, A. H.; Eisenberg, A. *Langmuir* **2003**, 19, 1001.
- (9) Terreau, O.; Luo, L. B.; Eisenberg, A. *Langmuir* **2003**, 19, 5601.
- (10) Terreau, O.; Bartels, C.; Eisenberg, A. *Langmuir* **2004**, 20, 637.
- (11) Dotera, T.; Hatano, A. *J. Chem. Phys.* **1996**, 105, 8413.
- (12) Bernardes, A. T. *Langmuir* **1996**, 12, 5763.
- (13) Noguchi, H.; Takasu, M. *Phys. Rev. E* **2001**, 64, 041913.
- (14) Yamamoto, S.; Maruyama, Y.; Hyodo, S. *J. Chem. Phys.* **2002**, 116, 5842.
- (15) Matsen, M. W. *Phys. Rev. Lett.* **1995**, 74, 4225.
- (16) Uneyama, T.; Doi, M. *Macromolecules* **2005**, 38, 5817.
- (17) Drolet, F.; Fredrickson, G. H. *Phys. Rev. Lett.* **1999**, 83, 4317.
- (18) Drolet, F.; Fredrickson, G. H. *Macromolecules* **2001**, 34, 5317.
- (19) Fredrickson, G. H.; Ganesan, V.; Drolet, F. *Macromolecules* **2002**, 35, 16.
- (20) Bohbot-Raviv, Y.; Wang, Z. G. *Phys. Rev. Lett.* **2000**, 85, 3428.
- (21) Tang, P.; Qiu, F.; Zhang, H. D.; Yang, Y. L. *J. Phys. Chem. B* **2004**, 108, 8434.
- (22) He, X. H.; Liang, H. J.; Huang, L.; Pan, C. Y. *J. Phys. Chem. B* **2004**, 108, 1931.
- (23) Wang, R.; Tang, P.; Qiu, F.; Yang, Y. L. *J. Phys. Chem. B* **2005**, 109, 17120.
- (24) Burke, S. E.; Eisenberg, A. *Polymer* **2001**, 42, 9111.
- (25) Shen, H. W.; Eisenberg, A. *Macromolecules* **2000**, 33, 2561.
- (26) Lynd, N. A.; Hillmyer, M. *Macromolecules* **2005**, 38, 8803.
- (27) Fredrickson, G. H.; Sides, S. W. *Macromolecules* **2003**, 36, 5415.
- (28) Sides, S. W.; Fredrickson, G. H. *J. Chem. Phys.* **2004**, 121, 4974.
- (29) Matsen, M. W.; Schick, M. *Curr. Opin. Colloid Interface Sci.* **1996**, 1, 329.
- (30) Thompson, R. B.; Matsen, M. W. *Phys. Rev. Lett.* **2000**, 85, 670.
- (31) Jiang, Y.; Chen, T.; Ye, F. W.; Liang, H. J.; Shi, A. C. *Macromolecules* **2005**, 38, 6710.
- (32) Edwards, S. F. *Proc. Phys. Soc.* **1965**, 85, 613.
- (33) Helfand, E. *J. Chem. Phys.* **1975**, 62, 999.